



This is a repository copy of *Quantitative Analysis of the Molecular Dynamics of P3HT:PCBM Bulk Heterojunction*.

White Rose Research Online URL for this paper:
<http://eprints.whiterose.ac.uk/124222/>

Version: Accepted Version

Article:

Guilbert, A.A.Y., Zbiri, M., Dunbar, A.D.F. orcid.org/0000-0002-2313-4234 et al. (1 more author) (2017) Quantitative Analysis of the Molecular Dynamics of P3HT:PCBM Bulk Heterojunction. *Journal of Physical Chemistry B*, 121 (38). pp. 9073-9080. ISSN 1520-6106

<https://doi.org/10.1021/acs.jpccb.7b08312>

Reuse

Items deposited in White Rose Research Online are protected by copyright, with all rights reserved unless indicated otherwise. They may be downloaded and/or printed for private study, or other acts as permitted by national copyright laws. The publisher or other rights holders may allow further reproduction and re-use of the full text version. This is indicated by the licence information on the White Rose Research Online record for the item.

Takedown

If you consider content in White Rose Research Online to be in breach of UK law, please notify us by emailing eprints@whiterose.ac.uk including the URL of the record and the reason for the withdrawal request.



eprints@whiterose.ac.uk
<https://eprints.whiterose.ac.uk/>

Quantitative Analysis of the Molecular Dynamics of P3HT:PCBM Bulk Heterojunction

Anne A. Y. Guilbert^{1}, Mohamed Zbiri^{2**}, Alan D.F. Dunbar³, Jenny Nelson¹*

¹ Centre for Plastic Electronics and Department of Physics, Blackett Laboratory, Imperial College London, London SW7 2AZ, United Kingdom.

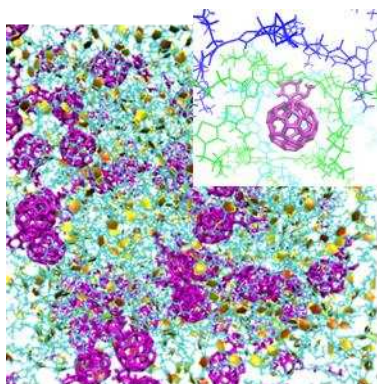
² Institut Laue-Langevin, 71 avenue des Martyrs, Grenoble Cedex 9, 38042, France.

³ Department of Chemical and Biological Engineering, the University of Sheffield, Sheffield S1 3JD, United Kingdom.

ABSTRACT. The optoelectronic properties of blends of conjugated polymers and small molecules are likely to be affected by the molecular dynamics of the active layer components. We study the dynamics of regio-regular poly(3-hexylthiophene) (P3HT): phenyl-C61-butyric acid methyl ester (PCBM) blends using molecular dynamics (MD) simulation on time scales up to 50 ns and in a temperature range of 250-360K. First, we compare the MD results with quasi-elastic neutron scattering (QENS) measurements. Experiment and simulation give evidence of the vitrification of P3HT upon blending, and the plasticization of PCBM by P3HT. Second, we reconstruct the QENS signal based on the independent simulations of the three phases constituting the complex microstructure of such blends. Finally, we found that P3HT chains tend to wrap around PCBM molecules in the amorphous mixture of P3HT and PCBM; this molecular

interaction between P3HT and PCBM is likely to be responsible for the observed frustration of P3HT, the plasticization of PCBM and the partial miscibility of P3HT and PCBM.

TOC GRAPHICS



KEYWORDS Conjugated polymer, fullerene, dynamics, modelling, quasi-elastic neutron scattering

Photocurrent generation in organic photovoltaic (OPV) devices occurs through a two-step process, involving the dissociation of photo-generated excitons into free charges at the interface between electron donating and electron accepting components – typically, a conjugated polymer and a fullerene derivative - and the transport of those free charges to the relevant electrodes.

The specific microstructure of the OPV active layer has been shown to impact these opto-electronic processes. The microstructure depends on the polymer:fullerene ratio, but also on the processing conditions.¹ In the case of a blend of a semi-crystalline polymer with fullerene, at fullerene concentrations below the miscibility limit of the fullerene with the polymer, the blend is composed of two phases consisting of nano-scale polymer crystalline domains embedded in an

amorphous mixture of polymer and fullerene.² Above this threshold, the fullerene phase separates resulting in a three phase microstructure.^{3,4}

Even below the glass transition temperature of polymers, relaxation processes of the side chains - used to solubilize polymers and small molecules for easy solution processing – take place on picoseconds to nanosecond time scales. This broad range of time scales are compatible with electronic processes such as charge separation, which has been shown to take place on sub-picosecond timescales.⁵ These structural dynamics are likely to modulate the dynamics and therefore the transfer of excitons and charges within the blend since energy and charge transfer are strongly dependent on local molecular packing. These structural dynamics are also important for mechanical stability of the materials: molecular motions are temperature-dependent and molecular diffusion becomes predominant above the glass transition of the polymer:fullerene blend leading to structural instabilities of the blends. This has been shown to be one of the degradation mechanisms of OPV devices.⁶ However, structural dynamics of OPV active layer are not well understood. This is the opportunity that we are trying to address in this letter. Building a robust model of the structural dynamics will make it possible to study the impact of these underlying structural disorder on the electronic processes.

In order to understand the structure-property relationship of OPV blends, recent studies have used molecular dynamics (MD) simulations to generate initial solid-state structures and extract molecular pairs to calculate transfer processes using quantum chemical methods.^{7,8} However, these structural models are hard to validate experimentally and the effect of the underlying molecular dynamics on the definition of pairs and on the transfer process is largely overlooked. The presence of another component in the blend may alter the conformation and the dynamics of

both polymer and small molecules compared to their behavior in neat samples through specific interactions at the molecular level.

A single glass transition temperature has been previously reported for P3HT:PCBM across a large range of composition. The observation of a single glass transition for the blend is consistent with the existence of a mixed amorphous phase of P3HT and PCBM as reported by Treat *et al.* and Leman *et al.*^{9,10} It should be noted that when applied to the P3HT:PCBM blend system the empirical Fox equation accurately describes the glass transition of P3HT:PCBM blends with a large amount of either P3HT or PCBM but fails for middle-range compositions,¹¹ which are of interest for OPV. In a previous study,¹² we probed the local dynamics of a blend of regioregular poly(3-hexylthiophene-2,5-diyl) (P3HT) and Phenyl-C61-butyric acid methyl ester (PCBM) at a 1:1 weight ratio on a time scale of 5 to 50 ps, using the time-of-flight quasi-elastic neutron scattering technique (QENS) over the temperature range 250-360K. The behavior of the QENS signal provided evidence on a time scale of 10s of ps for the frustration of P3HT upon blending with PCBM, especially above the glass transition temperature, and the plasticization of PCBM upon blending with P3HT. These observations are consistent with crystalline phases of P3HT and PCBM embedded in amorphous mixture of P3HT:PCBM. This three phases microstructure is the result of balanced interactions between polymer:polymer, fullerene:fullerene and polymer:fullerene.

If the experiment gives evidence of changes in dynamics due to partial miscibility of the two components, we could not answer the following questions: (i) what are the motions impacted upon blending on the measured time scale, which is directly relevant for charge generation? (ii) how P3HT and PCBM interact at the molecular level leading to these three phases microstructure and this frustration/plasticization upon blending?

In this letter, we use MD simulation to (i) study what particular motions (methyl rotation, reorientation of the side chains, backbone torsion, C₆₀ cage rotation, phenyl rotation) are observed on the time scale of our previous experiment (up to 50 ps) and (ii) investigate the specific interactions at the molecular level between PCBM and P3HT resulting in the observed P3HT frustration and PCBM plasticization upon blending. MD simulations allow us to study individually the different phases of the complex blend microstructure at the atomistic level, offering direct access to the different contributions to the QENS signal. Thus, in the present computational study, we consider crystalline P3HT, amorphous P3HT, crystalline PCBM, amorphous PCBM and an amorphous mixture of P3HT and PCBM. Although we measured blends with 50 wt% of PCBM, in this study, the simulated amorphous mixture of P3HT:PCBM contains 20 wt% of PCBM to take into account the finite miscibility of PCBM with P3HT, the other 80 wt% of PCBM being considered as crystalline. The miscibility limit of PCBM in P3HT has been estimated to be between 10 and 25 wt% by various groups^{2,9,13-14} and the model of the microstructure comprising solely a neat polymer and a neat fullerene phase has been ruled out experimentally in the favour of a three phase model with the fullerene being mixed with the polymer in the amorphous domain.² Phase separation is not achievable reachable within accessible time scales using fully atomistic MD simulations, thus the signal is reconstructed from the following three phases studied separately: crystalline P3HT, crystalline PCBM and the amorphous mixture leading to an overall PCBM loading of 50 wt%.

Previous studies have used MD simulations to study P3HT:PCBM microstructure and to investigate electronic processes at the interface. Carrillo *et al.*¹⁵ and Liu *et al.*¹⁶ assume that blends have a phase-separated microstructure with pure crystalline components and pure amorphous components. In all cases, they find that co-faciality between P3HT and PCBM is

favoured. This is also supported by DFT calculations.^{17,18} Lee *et al* used a coarse-grained approach to study thermal annealing at 150°C of P3HT:PCBM blend and used reverse mapping to fully atomistic representation. They showed that phase separation occurs at 1:1 weight ratio upon annealing but the resulting domains were not pure, supporting the three-phase model.¹⁹ Tummala *et al.*²⁰ have found using MD simulations that (i) the mechanism for mechanical failure of blends of P3HT and a fullerene derivative is that the polymer pulls away from the interface with the fullerene phase, creating voids and that (ii) the failure is dependent on the fullerene side chains, pointing towards specific molecular interactions between polymer and fullerene.

MD simulations were performed using the Gromacs-4.6.5 package,²¹⁻²³ where a leapfrog algorithm was adopted and periodic boundary conditions were applied in all directions. All the collection runs were carried out for 50 ns with a time step of 2 fs in NPT ensemble using a velocity-rescaling thermostat (time constant 0.1 ps) and a Berendsen barostat (1 bar, compressibility $4.5 \cdot 10^{-5} \text{ bar}^{-1}$, time constant 5 ps), The details regarding the preparation of the boxes, the force fields used and the equilibration protocols prior to the collection runs can be found in the Supporting Information.

Figure 1 compares the experimental¹² and simulated probability distribution functions $P(E, \tau, \beta)$, where E is the energy, τ the relaxation time and β the stretched exponent, of the relaxation times of the different degrees of freedom for neat protonated hydrogenated P3HT (h-P3HT) and for h-P3HT blended with deuterated PCBM (d-PCBM) (Figure 1 a-b) and for neat hydrogenated PCBM (h-PCBM) and for h-PCBM blended with deuterated P3HT (d-P3HT) (Figure 1 d-e), at 250K and 360K. The procedure to extract the relaxation times τ from the MD trajectories is

based on calculating the autocorrelation functions of the different degrees of freedom (cf. Supporting Information).

The simulation shows that the motions of some degrees of freedoms lie lower in energy than the experimental energy window of the IN6 spectrometer.¹² Thus, these motions are too slow to be resolved by the IN6 spectrometer and so are considered as elastic. Other motions lie higher in energy than the experimental energy window of the spectrometer. These motions are too fast to be resolved and thus, are contributing to the apparent background of the experiment.

As temperature increases, the maxima of the probability distribution functions shift to higher energies for all samples considered here, indicating a quickening of the motions. Thus, some motions such as the reorientation of h-P3HT side chains around the bond CT1-CT2 considered elastic at 250 K enters the energy window of the spectrometer at 360K and others such as the reorientation of the h-P3HT side chain around the bond CT4-CT5 becomes too fast to be resolved and thus, leave the energy window of the spectrometer.

Upon blending, both experimental and simulated probability distribution functions shift towards lower energies for h-P3HT while the opposite trend is found for h-PCBM, at 250 and 360K. The largest shift arises for h-PCBM at high temperature. This indicates that the motions of P3HT are slowed down while the motions of PCBM are quickened. In other words, upon blending P3HT becomes frustrated while PCBM is plasticized, which is in good agreement with the experiment. Modelling enabled us to conclude that it occurs for all degrees of freedom and on a longer time scale (up to 50 ns here).

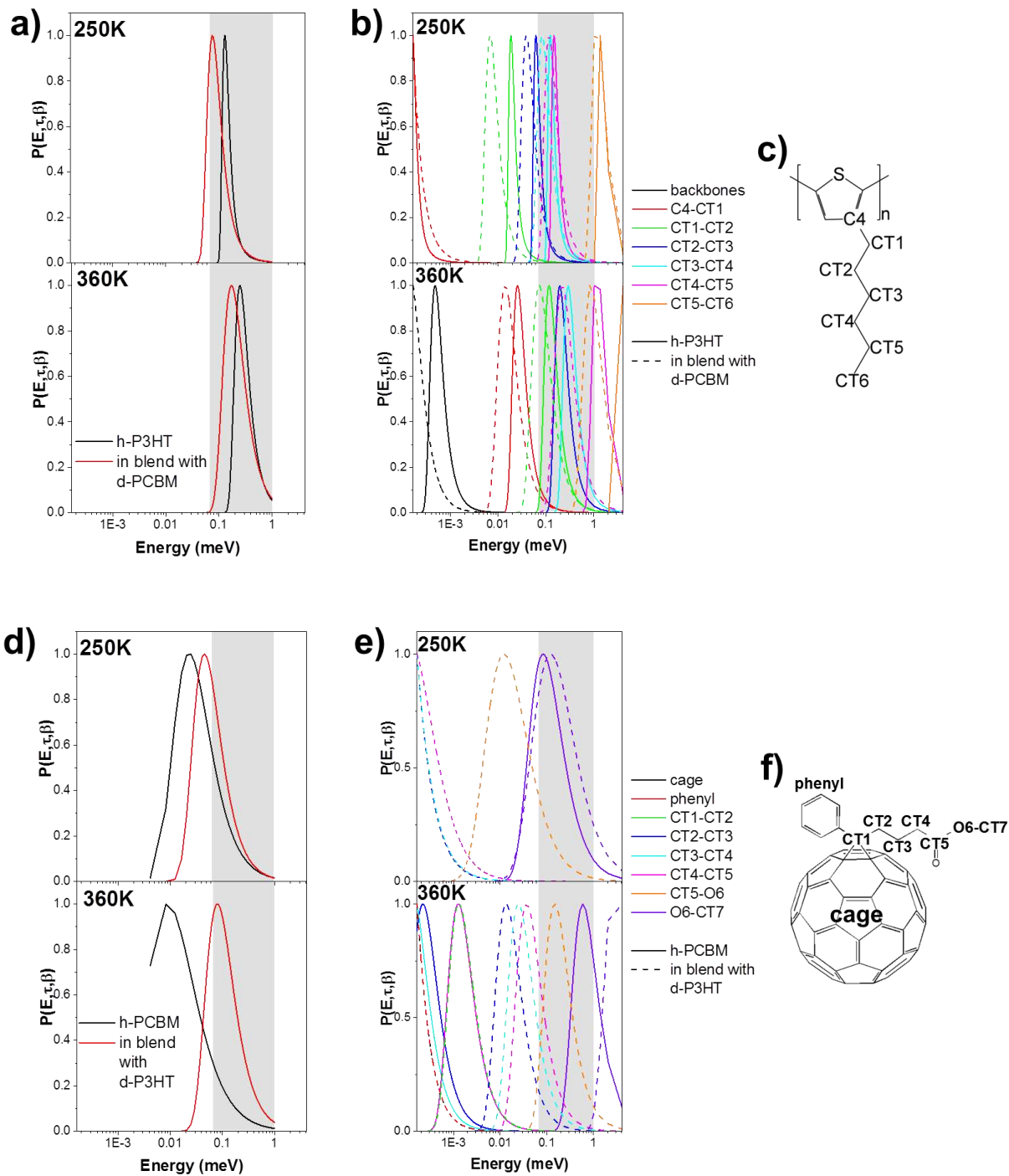


Figure 1. Experimental¹² probability distribution functions $P(E, \tau, \beta)$ of the relaxation times as a function of energy for (a) h-P3HT neat and blended with d-PCBM at 250K and 360K, and for (d) h-PCBM neat and blended with d-P3HT at 250K and 360K. Simulated probability distribution

functions $P(E, \tau, \beta)$ of the relaxation times of different degrees of freedom as a function of energy for (b) h-P3HT neat and blended with d-PCBM at 250K and 360K, and for (e) h-PCBM neat and blended with d-P3HT at 250K and 360K (e). The shaded area represents the instrumental energy window. (c) and (f) illustrate schematically the labels adopted for the different carbons belonging to the aliphatic chains of P3HT and PCBM, respectively, to help assigning plots in (b) and (e).

In order to compare simulation and experimental results, we should consider various aspects: (i) the experimental energy window and (ii) the different contributions to the signal stemming from the different phases of the neat samples (crystalline and amorphous) and blends (neat crystalline, and amorphous mixture) as well as (iii) the difference in incoherent neutron scattering cross-sections between components and between hydrogenated and deuterated molecules. As mentioned previously, in the simulation, we consider separately the three phases (crystalline P3HT, crystalline PCBM and an amorphous mixture of P3HT:PCBM) of the blend with experimental results for a blend of 1:1 weight ratio. The crystalline phase of P3HT accounts for about 20% by volume of the P3HT in the blend,²⁴ the miscibility of PCBM with P3HT is about 20 wt%^{2,9,13-14} and the rest consists of crystalline PCBM. For the blend of P3HT:PCBM with a 1:1 weight ratio considered here, this means that the crystalline P3HT phase accounts for 10 wt%, the amorphous P3HT phase accounts for 40 wt%, the amorphous PCBM phase accounts for 10 wt% and the crystalline PCBM phase accounts for 40 wt%. The PCBM-PCBM interactions are lowered by about 50% upon addition of 80 wt% of P3HT with comparable magnitude as P3HT:PCBM interactions (see **Table 1**); thus, PCBM is expected to be homogeneously dispersed in the amorphous P3HT matrix.

Table 1. Lennard-Jones potential energy per molecule for PCBM-PCBM, P3HT-P3HT and P3HT-PCBM for the neat and blend systems at 20 wt% PCBM loading. Note that we chose to consider P3HT tetramers as a molecule here to take into account the difference in number of atoms between a PCBM molecule and a 20-mer of P3HT. The PCBM-PCBM interactions are strongly lowered upon blending with comparable magnitude as the P3HT-PCBM interactions. This balance of interactions is indicative of PCBM being dispersed in the blend and low tendency to phase separate.

Lennard Jones potential energy per molecule (kJ/mol)				
	Neat		Blend	
	250K	360K	250K	360K
PCBM-PCBM	-194	-190	-89	-86
4-3HT-4-3HT	-121	-105	-108	-95
4-3HT-PCBM			-50	-45

The relaxation times for each degree of freedom within the different phases are provided in Supporting Information (Tables S2, S4, S6 and S8). A summary of the contributions of P3HT and PCBM in different phases to the measured QENS spectra of the overall systems is provided in **Figure 2**. The contributions are divided into elastic, quasi-elastic and apparent background as defined previously. Each contribution is weighted by its incoherent neutron-scattering cross-section.

It can be seen that a very few degrees of freedom fall within the time window of IN6. P3HT is predominantly amorphous. Recent papers estimated its crystallinity to account for ~20% by volume of the P3HT phase in blend films.²⁴ Therefore, the QENS spectra are dominated by the

amorphous behavior of P3HT in the neat h-P3HT sample. Because of the difference in incoherent neutron scattering cross-section between h-P3HT and d-PCBM and because of the finite miscibility of P3HT with PCBM, the QENS spectra of h-P3HT:d-PCBM sample is also dominated by P3HT behavior in the amorphous mixture. PCBM neat samples are largely crystalline, thus most of the QENS signal results from the scattering of the crystalline phase. The difference in cross-section between d-P3HT and h-PCBM results in the QENS signal dominated by h-PCBM dynamics. However, the low miscibility of PCBM with P3HT leads to a weak signal from the amorphous mixture of the d-P3HT:h-PCBM sample. Although the difference in relaxation times between neat PCBM and blended PCBM in the amorphous mixture is quite large, this is only slightly reflected in the QENS spectra.

Based solely on the analysis of the experimental data, we could not differentiate between two models for the observed motions: (i) localized motions, thus the relaxation times are Q-independent and (ii) jump diffusion within a sphere, thus the relaxation times are Q-dependent. Q refers here to the norm of the scattering vector. Using molecular dynamics simulation, we can study both the time and the space spanned by the various degrees of freedom of the molecules. The spatial distribution functions of the degrees of freedom within the experimental time window are depicted in Figure S13. The spatial distribution functions show that the motions sample a large volume of the space during the simulations, suggesting that the jump diffusion model is adequate to fit the QENS data for P3HT dynamics at all temperatures and PCBM dynamics in the blend at high temperature. At low temperature, PCBM motions are confined and the localized motions model is thus adequate.

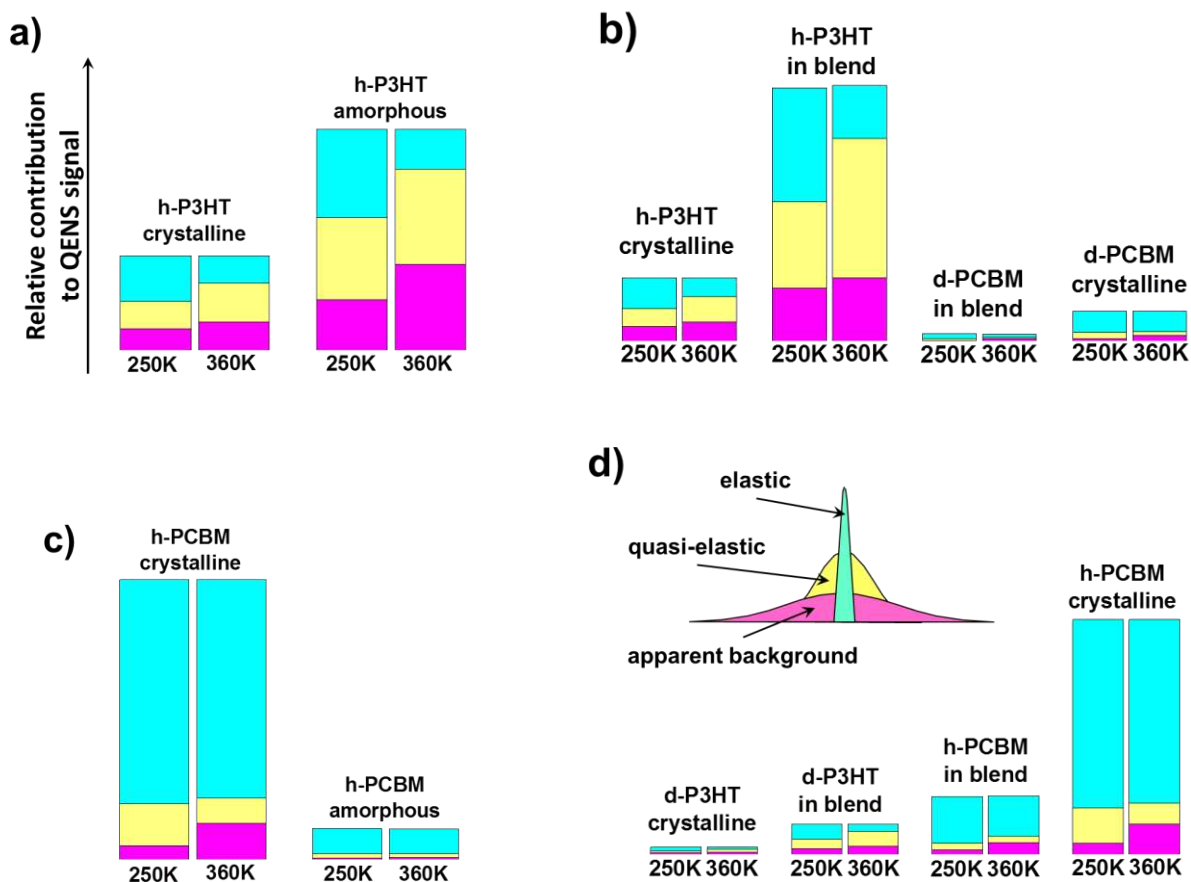


Figure 2. Contributions of the different phases of P3HT and PCBM to the elastic (cyan), quasi-elastic (yellow) and apparent background (magenta) components of the IN6 QENS spectra at 250K and 360K in neat samples (a and c) and in blends (b and d). The column heights are chosen to represent the weight fraction of the different phases in the neat sample and in blends with 1:1 weight ratio. The contributions are further weighted by the difference in terms of incoherent cross sections of h-P3HT, h-PCBM, d-P3HT and d-PCBM. The crystallinity of both components decreases upon blending as can be seen by XRay diffraction (Figure S14 Supporting Information).

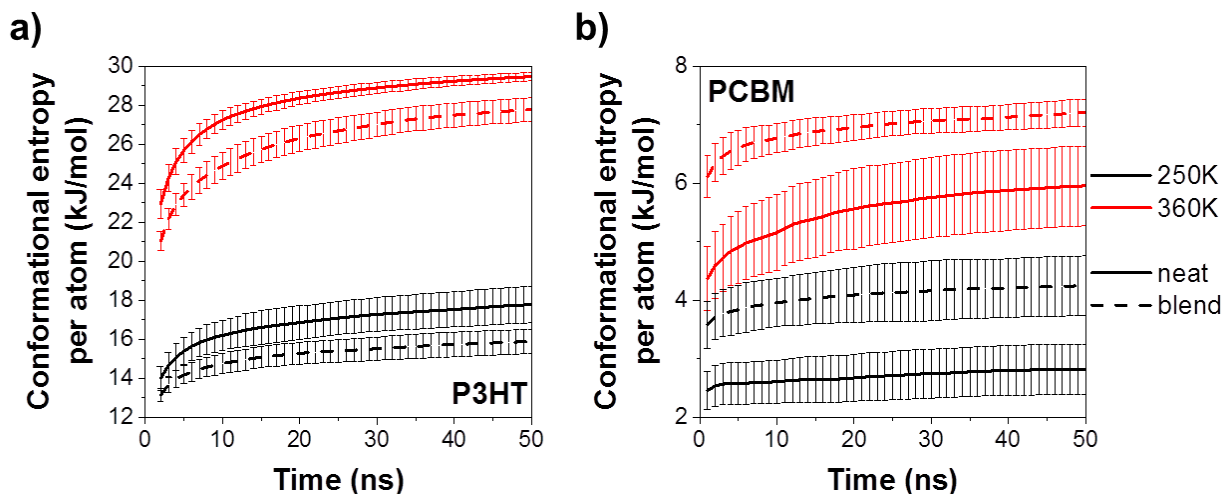


Figure 3. Conformational entropy of (a) P3HT and (b) PCBM in neat (solid line) amorphous sample and in amorphous blend (dashed line).

In order to investigate the microscopic reasons for the observed frustration of P3HT and plasticization of PCBM, we calculated the conformational entropy (cf. Supporting Information) of both P3HT and PCBM in neat amorphous samples and in the amorphous blend. **Figure 3** shows that P3HT frustration can be explained by a decrease in the conformational entropy upon blending, while PCBM plasticization can be related to an increase in the conformational entropy upon blending with P3HT; in both cases this would occur both below and above the glass transition of P3HT. The glass transition of P3HT and PCBM are around 275K and 400K respectively.²⁵⁻²⁶ Note that the glass transition temperature is not well defined in the literature since its determination depends on the molecular weight and on the technique used for measuring the transition.^{11,27} In the case of P3HT, the increase of the conformational entropy with temperature is much larger than the change upon blending but it is of the same order of magnitude in the case of PCBM. The slight decrease in entropy of P3HT upon blending is consistent with a reduced flexibility of P3HT upon blending, inhibiting the molecules ability to

sample new configurations during the simulation. This can be directly correlated with a 4.5% decrease in free volume relative to the neat sample for P3HT at 250K, and a decrease of 5.4 % upon blending at 360K. For PCBM, an increase in free volume of 18% and 28% upon blending relative to the neat sample at 250K and 360K respectively is found.

We study the impact of PCBM on P3HT conformation by looking at the relative arrangement of the two molecules in the blend. The snapshot in Figure 4 (a) suggests that the P3HT chain tends to wrap around the PCBM molecule. To quantify this behavior, we define the angle θ (Figure 4 (b)) as the angle formed by two vectors $\mathbf{v1}$ and $\mathbf{v2}$, where $\mathbf{v1}$ is the vector linking the center of mass of PCBM cage and the center of the thiophene ring and $\mathbf{v2}$ is the vector normal to the thiophene ring. The order parameter $\langle 3\cos^2(\theta)-1 \rangle$ is equal to 2 if the thiophene ring is co-facial with the PCBM cage surface, -1 if the thiophene ring sits perpendicular to the PCBM cage surface and 0 if all orientations are equally likely. Here, a first layer of ordered thiophene rings is clearly observed within a distance of 7 to 10 Å from the center of mass of the PCBM cage, corresponding to a distance between the cage surface and the P3HT thiophene ring of 3.5-4.5 Å. This short distance illustrates the strength of the interaction between PCBM and P3HT. This first layer corresponds to the first peak of the radial distribution function of P3HT monomers around PCBM. The order is lost at longer distances.

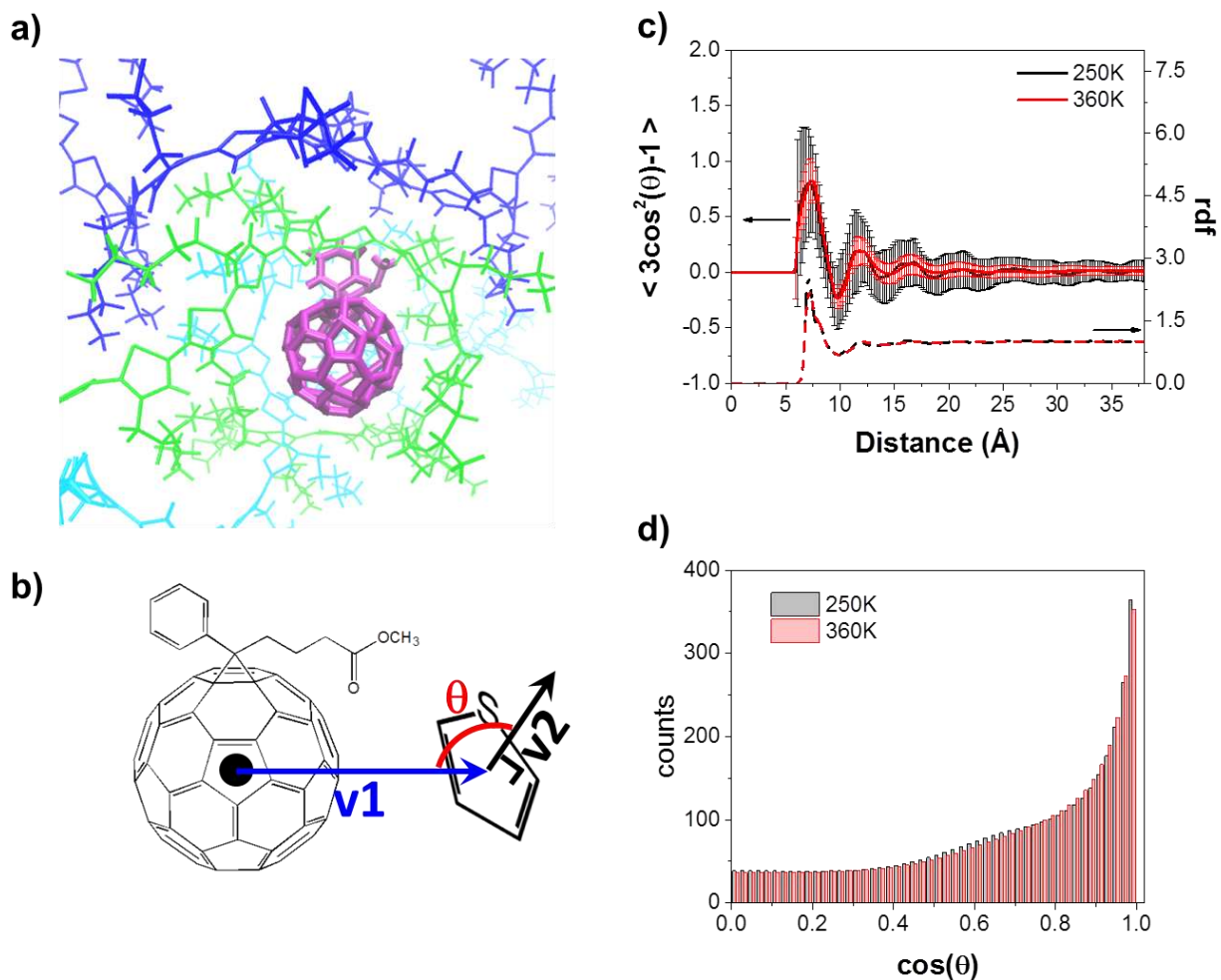


Figure 4. (a) MD snapshot of P3HT wrapped around PCBM. (b) Definition of the angle θ formed by two vectors $\mathbf{v1}$ and $\mathbf{v2}$, where $\mathbf{v1}$ is the vector linking the center of mass of PCBM cage and the center of the thiophene ring and $\mathbf{v2}$ is the vector normal to the thiophene ring. (c) The order parameter defined as $\langle 3\cos^2(\theta) - 1 \rangle$, and a radial distribution function (rdf) as a function of the distance from the center of mass of C60 cage. (d) Distribution of $\cos(\theta)$ within 5 and 10 Å of the center of mass of C60 cage.

We observe this partial wrapping effect on the four blends we study in this paper h-P3HT:h-PCBM, d-P3HT:h-PCBM, h-P3HT:d-PCBM and d-P3HT:d-PCBM that have been prepared from different random starting point. This partial wrapping effect is also stable with temperature,

thus we do believe that this is not an artefact from the simulation. Furthermore, wrapping of analogue systems have already been observed. For instance, conjugated polymers have already been observed wrapping around carbon nanotubes²⁸ and it has been shown that this wrapping mechanism stabilized carbon nanotube dispersions and that it was influenced by the presence of sulfur in the polymer and by the radius of the carbon nanotube.²⁹ Also, supramolecular crown ether and metal complex with corannulene derivative ligands have also been shown to embrace C₆₀ fullerene.³⁰⁻³¹ Previous MD studies on P3HT:PCBM^{15-16,20} have focused on modelling adjacent slabs of pure P3HT and pure PCBM while experimental studies evidence the presence of an amorphous mixture of P3HT and PCBM.² The wrapping effect has not been observed due to the constrained molecular arrangement in adjacent slab. However, evidence of co-faciality in the blend, which is also compatible with wrapping, has already been reported both experimentally using time-resolved electron paramagnetic resonance method³²⁻³³ and using simulations at the interface between P3HT and PCBM layers.¹⁵⁻¹⁸

The wrapping of P3HT leads to a frustration of P3HT backbone movement since the possible conformation to be adopted is restrained. Also, the side chains are pushed outside of the complex C₆₀-thiophene and lead to a restriction of the free volume in which they can evolve, thus leading to a frustration of all rotational movements along the side chains. On the contrary, this wrapping effect stabilizes individual PCBM in the blend. The lower density of the packing of the polymer leads to enhance mobility for PCBM and leads to the observed plasticization effect. This stabilization of individual PCBM in the blend is limited to a certain range of composition but is likely to be promoting the partial miscibility previously observed for P3HT and PCBM.

In conclusion, studying the different phases of the 3-phase microstructure of OPV active layer by MD simulations enabled us to identify the molecular motions within the different phases

captured by our previous experiment using IN6 spectrometer and to rationalize the observed P3HT frustration and PCBM plasticization by P3HT wrapping itself around PCBM molecule in the amorphous mixture. We studied the contributions from the various degrees of freedom from both P3HT and PCBM within different phases (crystalline, amorphous and amorphous mixture) and showed that within the amorphous mixture, the dynamics of the reorientation of P3HT side chains are inhibited by the presence of PCBM and the dynamics of PCBM side chains are found to be quickened when blended with P3HT on the time scale of our previous experiment (up to 50 ps). MD enabled us to study P3HT and PCBM dynamics on longer time scale (up to 50 ns) and we found that the observed frustration of P3HT and plasticization of PCBM can be extended to motions that were not captured by IN6 spectrometer. These trends are consistent with changes in the free volume available for conformational fluctuation upon blending.

We showed that the observed P3HT frustration and PCBM plasticization behaviors are due to specific interactions between P3HT and PCBM in the amorphous mixture. P3HT wraps itself around PCBM with the thiophene being co-facial to PCBM. It has been shown that miscibility is a parameter controlling the fill factor of OPV devices³⁴ but also their microstructural stability.^{13,35} Such polymer arrangement with monomers co-facial to the small molecule acceptor are also likely to be beneficial for charge transfer and thus, charge generation. Thus, we speculate that the knowledge of such specific interactions can lead to the design and selection of small molecule acceptors to improve morphological robustness. Adding more side chains to the fullerene cage or replacing the linear side chain of PCBM with bulkier and longer side chains is likely to inhibit the wrapping effect of conjugated polymer and leads to lower interactions between the polymer and the fullerene. This has already been evidenced for the bis and tris adduct of PCBM by differential scanning calorimetry,³⁶ and replacing PCBM side chain has been

proven an effective method to reduce the fullerene miscibility with poly(3-hexylselenophene), P3HS.³⁴ Recently, advances have been made in the synthesis of non-fullerene acceptors.³⁷ A trade-off between planarity and miscibility has to be reached in order to create a suitable blend microstructure for efficient OPV devices. Planarity is believed to enhance charge transport but unfavorably large aggregates of the non-fullerene acceptors have been observed.³⁸⁻³⁹ Strategies to overcome large aggregation include the design of molecules featuring a large intramolecular twist.⁴⁰ We speculate that tuning the interaction between the polymer backbone and the non-fullerene acceptor can inhibit the large phase separation. Combined QENS and MD studies of blends of conjugated polymers with such new acceptors could therefore be valuable.

ASSOCIATED CONTENT

The Supporting Information contains details of the MD simulations including the force fields, the calculated dihedral order parameters and dihedral distribution functions, autocorrelation functions, the extracted relaxation times, the probability distribution functions $P(E, \tau, \beta)$ of the relaxation times, grazing incidence X-ray diffraction data, and spatial distribution functions.

AUTHOR INFORMATION

Corresponding Author

*Email: a.guilbert09@imperial.ac.uk; Phone: +(44) (0)2075947563

**Email: zbiri@ill.fr; Phone: +33 (0)4 76 20 7803

ACKNOWLEDGMENT

A.G. acknowledges the Thomas Young Centre under Grant Number TYC-101 – EP/N50869X/1. A.G. and J.N. acknowledge ESPRC (EP/P005543/1). We thank the Imperial College High

Performance Computing Service (doi: 10.14469/hpc/2232). We thank Diamond Light Source for access to beamline I07 (Proposal Number: Si15486-1) that contributed to the results presented here and we acknowledge Dr Tom Arnold and Prof. Chris Nicklin for their help.

REFERENCES

1. Treat, N. D.; Chabynyc, M. L. Phase separation in bulk heterojunctions of semiconducting polymers and fullerenes for photovoltaics. *Annu. Rev. Phys. Chem.* **2014**, *65*, 59-81.
2. Yin, W.; Dadmun, M. A New Model for the Morphology of P3HT/PCBM Organic Photovoltaics from Small-Angle Neutron Scattering: Rivers and Streams. *ACS Nano*. **2011**, *5*, 4756-4768.
3. Watts, B.; Belcher, W. J.; Thomsen, L.; Ade, H.; Dastoor, P. C. A Quantitative Study of PCBM Diffusion during Annealing of P3HT:PCBM Blend Films. *Macromolecules* **2009**, *42*, 8392-8397.
4. Müller, C.; Ferenczi, T. A. M.; Campoy-Quiles, M.; Frost, J. M.; Bradley, D. D. C.; Smith, P.; Stingelin-Stutzmann, N.; Nelson, J. Binary Organic Photovoltaic Blends: A Simple Rationale for Optimum Compositions. *Adv. Mater.* **2008**, *20*, 3510-3515.
5. Gao, F.; Inganäs, O. Charge generation in polymer-fullerene bulk-heterojunction solar cells. *Phys. Chem. Chem. Phys.* **2014**, *16*, 20291-304.
6. Bertho, S.; Janssen, G.; Cleij, T. J., Conings, B.; Moons, W.; Gadisa, A.; D'Haen, J.; Goovaerts, E.; Lutsen, L.; Manca, J.; Vanderzande, D. Effect of temperature on the morphological and photovoltaic stability of bulk heterojunction polymer:fullerene solar cells. *Sol. Energy Mater. Sol. Cells* **2008**, *92*, 753-760.

7. Castet, F.; D'Avino, G.; Muccioli, L.; Cornil, J.; Beljonne, D. Charge separation energetics at organic heterojunctions: on the role of structural and electrostatic disorder. *Phys. Chem. Chem. Phys.* **2014**, *16*, 20279-90.
8. Poelking, C.; Daoulas, K.; Troisi, A.; Andrienko, D. Morphology and Charge Transport in P3HT: A Theorist's Perspective. *Adv. Polym. Sci.* **2014**, *265*, 139-180.
9. Treat, N. D.; Brady, M. A.; Smith, G.; Toney, M. F.; Kramer, E. J.; Hawker, C. J.; Chabynyc, M. L. Interdiffusion of PCBM and P3HT Reveals Miscibility in a Photovoltaically Active Blend. *Adv. Energy Mater.* **2011**, *1*, 82-89.
10. Leman, D.; Kelly, M. A.; Ness, S.; Engmann, S.; Herzing, A.; Snyder, C.; Ro, H. W.; Kline, R. J.; DeLongchamp, D. M.; Richter, L. J. In Situ Characterization of Polymer–Fullerene Bilayer Stability. *Macromolecules* **2015**, *48*, 383-392.
11. Müller, C. On the glass transition of polymer semiconductors and its impact on polymer solar cell stability. *Chem. Mater.* **2015**, *27*, 2740-2754.
12. Guilbert, A. A. Y.; Zbiri, M.; Jenart, M. V. C.; Nielsen, C. B.; Nelson, J. New Insights into the Molecular Dynamics of P3HT:PCBM Bulk Heterojunction: A Time-of-Flight Quasi-Elastic Neutron Scattering Study. *J. Phys. Chem. Lett.* **2016**, *7*, 2252-2257.
13. Collins, B. A.; Tumbleston, J. R.; Ade, H. Miscibility, Crystallinity, and Phase Development in P3HT/PCBM Solar Cells: Toward an Enlightened Understanding of Device Morphology and Stability. *J. Phys. Chem. Lett.* **2011**, *2*, 3135-3145.
14. Guilbert, A. A. Y.; Schmidt, M.; Bruno, A.; Yao, J.; King, S.; Tuladhar, S. M.; Kirchartz,

- T.; Alonso, M. I.; Goñi, A. R.; Stingelin, N.; Haque, S. A.; Campoy-Quiles, M.; Nelson, J. Spectroscopic Evaluation of Mixing and Crystallinity of Fullerenes in Bulk Heterojunctions. *Adv. Funct. Mater.* **2014**, *24*, 6972–6980.
15. Carrillo, J.-M. Y.; Seibers, Z.; Kumar, R.; Matheson, M. A.; Ankner, J. F.; Goswami, M.; Bhaskaran-Nair, K.; Shelton, W. A.; Sumpter, B. G.; Kilbey, S. M. Petascale Simulations of the Morphology and the Molecular Interface of Bulk Heterojunctions. *ACS Nano* **2016**, *10*, 7008-7022.
 16. Liu, T.; Cheung, D. L.; Troisi, A. Structural variability and dynamics of the P3HT/PCBM interface and its effects on the electronic structure and the charge-transfer rates in solar cells. *Phys. Chem. Chem. Phys.* **2011**, *13*, 21461.
 17. Li, L.-H.; Kontsevoi, O. Y.; Freeman, A. J. Orientation-Dependent Electronic Structures and Optical Properties of the P3HT:PCBM Interface: A First-Principles GW-BSE Study. *J. Phys. Chem. C* **2014**, *118*, 10263-10270.
 18. Marchiori, C. F. N.; Koehler, M. Density functional theory study of the dipole across the P3HT : PCBM complex: the role of polarization and charge transfer. *J. Phys. D. Appl. Phys.* **2014**, *47*, 215104.
 19. Lee, C.-K.; Pao, C.-W.; Chu, C.-W. Multiscale molecular simulations of the nanoscale morphologies of P3HT:PCBM blends for bulk heterojunction organic photovoltaic cells. *Energy & Environmental Science* **2011**, *4*, 4124.
 20. Tummala, N. R.; Bruner, C.; Risko, C.; Brédas, J.-L.; Dauskardt, R. H. Molecular-Scale Understanding of Cohesion and Fracture in P3HT:Fullerene Blends. *ACS Appl. Mater.*

Interfaces **2015**, 7, 9957-9964.

21. Berendsen, H. J. C.; van der Spoel, D.; van Drunen, R. GROMACS: A message-passing parallel molecular dynamics implementation. *Comput. Phys. Commun.* **1995**, 91, 43-56.
22. Van Der Spoel, D.; Lindahl, E.; Hess, B.; Groenhof, G.; Mark, A. E.; Berendsen, H. J. C. GROMACS: Fast, flexible, and free. *J. Comput. Chem.* **2005**, 26, 1701-1718.
23. Hess, B.; Kutzner, C.; van der Spoel, D.; Lindahl, E. GROMACS 4: Algorithms for Highly Efficient, Load-Balanced, and Scalable Molecular Simulation. *J. Chem. Theory Comput.* **2008**, 4, 435–447.
24. Etampawala, T.; Ratnaweera, D.; Morgan, B.; Diallo, S.; Mamontov, E.; Dadmun, M. Monitoring the dynamics of miscible P3HT:PCBM blends: A quasi elastic neutron scattering study of organic photovoltaic active layers. *Polymer* **2015**, 61, 155-162.
25. Zhao, J.; Swinnen, A.; Van Assche, G.; Manca, J.; Vanderzande, D.; Van Mele, B. Phase diagram of P3HT/PCBM blends and its implication for the stability of morphology. *J. Phys. Chem. B* **2009**; 113, 1587-1591.
26. Abad, J.; Espinosa, N.; Ferrer, P.; García-Valverde, R.; Miguel, C.; Padilla, J.; Alcolea, A.; Castro, G. R.; Colchero, J.; Urbina, A. Molecular structure of poly(3-alkyl-thiophenes) investigated by calorimetry and grazing incidence X-ray scattering. *Sol. Energy Mater. Sol. Cells* **2012**, 97, 109-118.
27. Root, S. E.; Alkhadra, M. A.; Rodriguez, D.; Printz, A. D.; Lipomi, D. J.. Measuring the Glass Transition Temperature of Conjugated Polymer Films with Ultraviolet–Visible Spectroscopy. *Chem. Mater.* **2017**, 29, 2646-2654.

28. Fujigaya, T.; Nakashima, N. Non-covalent polymer wrapping of carbon nanotubes and the role of wrapped polymers as functional dispersants. *Sci. Technol. Adv. Mater.* **2015**, *16*, 24802.
29. Zaminpayma, E.; Mirabbaszadeh, K. Investigation of molecular interaction between single-walled carbon nanotubes and conjugated polymers. *Polym. Compos.* **2012**, *33*, 548-554.
30. Nierengarten, J.-F.; Guldi, D. M.; Ortí, E.; Martín, N.; Moreira, L.; In Calbo, J.; Krick Calderon, R. M.; Santos, J. E.; Illescas, B. M.; Ara, J.; Or, E.; Mar, N. Chemical Science Unveiling the nature of supramolecular crown ether–C₆₀ interactions. *Chem. Sci.* **2015**, *6*, 4377-5094.
31. Álvarez, C. M.; García-Escudero, L. A.; García-Rodríguez, R.; Martín-Álvarez, J. M.; Miguel, D.; Rayón, V. M. Dalton Transactions An international journal of inorganic chemistry Enhanced association for C₇₀ over C₆₀ with a metal complex with corannulene derivate ligands. *Dalt. Trans.* **2014**, *43*, 15659-16116.
32. Kobori, Y.; Noji, R.; Tsuganezawa, S. Initial Molecular Photocurrent: Nanostructure and Motion of Weakly Bound Charge-Separated State in Organic Photovoltaic Interface. *J. Phys. Chem. C* **2013**, *117*, 1589-1599.
33. Kobori, Y.; Miura, T. Overcoming Coulombic Traps: Geometry and Electronic Characterizations of Light-Induced Separated Spins at the Bulk Heterojunction Interface. *J. Phys. Chem. Lett.* **2015**, *6*, 113-123.
34. Treat, N. D.; Varotto, A.; Takacs, C. J.; Batara, N.; Al-Hashimi, M.; Heeney, M. J.; Heeger, A. J.; Wudl, F.; Hawker, C. J.; Chabynyc, M. L. Polymer-fullerene miscibility: a metric for screening new materials for high-performance organic solar cells. *J. Am. Chem.*

Soc. **2012**, *134*, 15869-79.

35. Müller, C.; Bergqvist, J.; Vandewal, K.; Tvingstedt, K.; Anselmo, A. S.; Magnusson, R.; Alonso, M. I.; Moons, E.; Arwin, H.; Campoy-Quiles, M.; Inganäsa, O. Phase behaviour of liquid-crystalline polymer/fullerene organic photovoltaic blends: thermal stability and miscibility. *J. Mater. Chem.* **2011**, *21*, 10676.
36. Guilbert, A. A. Y.; Reynolds, L.X.; Bruno, A.; MacLachlan, A.; King, S. P.; Faist, M. A.; Pires, E.; Macdonald, J. E.; Stingelin, N.; Haque, S. A.; Nelson, J. Effect of multiple adduct fullerenes on microstructure and phase behavior of P3HT:fullerene blend films for organic solar cells. *ACS Nano* **2012**; *6*, 3868-75.
37. Chen, W.; Zhang, Q.; Lin, Y.Z.; Wang, W. B.; Gao, M. L.; Li, L. L.; Zhang, J.; Zhan, X. W.; Lee, T. H.; Huang, M. J.; Choi, H. S.; Kim, J. Y.; Choy, W. C. H.; Sun, Y. M.; Yan, H.; Loo, Y. L.; Ng, F.; Zhu, X. Y.; Nuckolls, C.. Recent progress in non-fullerene small molecule acceptors in organic solar cells (OSCs). *J. Mater. Chem. C* **2017**, *5*, 1275-1302.
38. Jiang, X.; Xu, Y.; Wang, X.; Wu, Y.; Feng, G.; Li, C.; Ma, W.; Li, W.; Wang, C.; Howard, P.; Li, W.; Li, W.; Ma, W.; Li, W.; Gao, F.; Wei, Z.; Ma, W.; Wang, C.; Hodgkiss, J.; Bo, Z.; Inganäs, O.; Li, Y.; Zhan, X. Non-fullerene organic solar cells based on diketopyrrolopyrrole polymers as electron donors and ITIC as an electron acceptor. *Phys. Chem. Chem. Phys.* **2017**, *19*, 8069-8075.
39. Zhang Z, Li M, Liu Y, et al. Simultaneous enhancement of the molecular planarity and the solubility of non-fullerene acceptors: effect of aliphatic side-chain substitution on the photovoltaic performance. *J. Mater. Chem. A* **2017**; *5*(17):7776-7783.

40. Nielsen CB, Holliday S, Chen H-Y, Cryer SJ, McCulloch I. Non-Fullerene Electron Acceptors for Use in Organic Solar Cells. *Acc. Chem. Res.* 2015;48(11):2803-2812.